Limited proteolysis of a disulfide-linked apoA-I dimer in reconstituted HDL

Laura Calabresi,* Gabriella Tedeschi,† Chiara Treu,† Severino Ronchi,† Debora Galbiati,* Silvia Airoldi,* Cesare R. Sirtori,* Yves Marcel,§ and Guido Franceschini[1,*]

Center E. Grossi Paoletti,* Department of Pharmacological Sciences, University of Milano, 20133 Milano, Italy; Institute of Veterinary Physiology and Biochemistry,† University of Milano, 20133 Milano, Italy; and Lipoprotein and Atherosclerosis Group,§ University of Ottawa Heart Institute, Ontario, Canada K1Y 4W7

Abstract The apolipoprotein A-I$_{Milano}$ (apoA-I$_M$) is a molecular variant of apoA-I characterized by the Arg^{173}→Cys substitution, leading to the formation of homodimers A-I$_M$/A-I$_M$. Upon interaction with palmitoyloleoylphosphatidylcholine, A-I$_M$/A-I$_M$ forms only two species of reconstituted HDL (rHDL) particles, with diameters of 7.8 and 12.5 nm. We used limited proteolysis to analyze the conformation of A-I$_M$/A-I$_M$ in the two rHDL particles, in comparison with that of apoA-I in rHDL of similar size. ApoA-I in the small, 7.8-nm rHDL is degraded to a greater extent (50% after 6 h) than in the large rHDL (<10% degraded after 6 h). The protease susceptibility of A-I$_M$/A-I$_M$ in small and large rHDL is instead remarkably the same, with A-I$_M$/A-I$_M$ being much more sensitive to proteolytic digestion (50% degraded after 10 min) than apoA-I. The identification of the proteolytic fragments by immunoblotting, N-terminal sequencing, and molecular mass determination, shows that the N-terminus of both proteins is resistant to proteolysis, with six cleavage sites located in the central and carboxy-terminal portions of the molecules. Cleavage in the middle of apoA-I occurs at distinct sites in 7.8-nm (Lys^{118}) and 12.7-nm (Arg^{123}) rHDL, indicating a different conformation in small and large rHDL particles. The A-I$_M$/A-I$_M$ instead adopts a unique and identical conformation in small and large rHDL, with the carboxy-terminal portion of the molecule being remarkably more accessible to the proteases than in apoA-I. This suggests the presence of a novel carboxy-terminal domain in A-I$_M$/A-I$_M$, not organized in a compact structure and not shared by wild-type apoA-I, which may account for the unique functional properties of A-I$_M$/A-I$_M$.—Calabresi, L., G. Tedeschi, C. Treu, S. Ronchi, D. Galbiati, S. Airoldi, C. R. Sirtori, Y. Marcel, and G. Franceschini. **Limited proteolysis of a disulfide-linked apoA-I dimer in reconstituted HDL. *J. Lipid Res.* 2001.** 42: **935–942.**

Supplementary key words limited proteolysis • protein conformation • apolipoprotein A-I$_{Milano}$

Apolipoprotein A-I (apoA-I) is the major protein constituent of human HDL, and is believed to be responsible for the antiatherogenic and antithrombogenic properties of HDL (1). Indeed, apoA-I overexpression in transgenic mice and rabbits increases the number of circulating HDL particles and protects the animals from the development of diet- or gene-induced atherosclerosis (2–4). Moreover, adenovirus-mediated transfer of the apoA-I gene into apoE-deficient mice remarkably inhibits neointima formation after endothelial denudation (5), suggesting a direct protective effect of apoA-I on the arterial wall. A number of mechanisms, including facilitation of reverse cholesterol transport (6), prostacyclin stabilization (7), activation of fibrinolysis (8), and modulation of cell-cell interactions (9), have been proposed to explain this protective effect. The structural requirements for these different functions in atherosclerosis protection are mostly unknown.

ApoA-I is synthesized both in the liver and in the intestine as pre-pro-apoA-I, and is then processed to the mature form of 243 residues (10). ApoA-I is predicted to consist of a series of eight 22 amino acids, proline punctuated, amphipathic α-helices, and two 11 amino acids tandem repeats (11–13). The recent crystallization of a large fragment of apoA-I lacking the N-terminal 43 residues provided the first direct information on the three-dimensional structure of the lipid-free molecule (14). According to these data, the protein adopts a continuously curved conformation, with a horseshoe-like shape due to the presence of kinks at the site of proline residues (14).

Upon interaction with phospholipids, apoA-I generates a number of discretely sized discoidal particles resembling nascent HDL, also known as reconstituted HDL (rHDL) (15). These rHDL mimic most of the physiological properties of plasma HDL and proved to be a valuable tool in identifying structural requirements for some HDL func-

Abbreviations: ApoA-I, apolipoprotein A-I; rHDL, reconstituted HDL; apoA-I$_M$, apolipoprotein A-I$_{Milano}$; A-I$_M$/A-I$_M$, A-I$_M$ homodimer; POPC, palmitoyloleoylphosphatidylcholine; GGE, gradient gel electrophoresis; DMS, dimethylsuberimidate; CD, circular dichroism; mAbs, monoclonal antibodies.

[1] To whom correspondence should be addressed at the Center E. Grossi Paoletti, Department of Pharmacological Sciences, Via Balzaretti 9 20133, Milano, Italy.
e-mail: Guido.Franceschini@unimi.it

tions (9, 16–18). Well-defined rHDL made with apoA-I and synthetic phosphatidylcholines, and with specific ratios between the components, have very reproducible sizes and compositions (15). The rHDL particles can be grouped into classes according to the number of apoA-I molecules per particle, and within each class into particles of different sizes. These subclasses are thought to arise from different apoA-I conformations, reflecting the number of amphipathic helices in contact with lipids on the edge of the disc (19). Two models have been proposed for the structure of apoA-I around the periphery of the rHDL discs. The "belt" model describes apoA-I organization in terms of the X-ray structure, with two molecules of apoA-I forming a pair of continuous amphipathic helices parallel to the plane of the disc (14, 20, 21). In the "picket-fence" model, the amphipathic helices of apoA-I arrange into tightly packed antiparallel segments, oriented perpendicular to the plane of the disc (22, 23).

The apoA-I_{Milano} (apoA-I_M) has been the first described molecular variant of human apolipoproteins (24). The apoA-I_M differs from wild-type apoA-I for an Arg^{173}→Cys substitution, leading to the formation of disulfide-linked dimers (25). Although the structure of the lipid-free and lipid-bound apoA-I_M monomer differs only slightly from wild-type apoA-I (26), the introduction of an interchain disulfide bridge in the apoA-I_M homodimer (A-I_M/A-I_M) remarkably alters the physico-chemical properties of apoA-I (27). When compared with apoA-I, the lipid-free A-I_M/A-I_M displays a higher α-helical content and a more folded tertiary structure (27). Upon interaction with phospholipids, A-I_M/A-I_M forms only two species of rHDL with a diameter of 7.8 and 12.5 nm, which contain one or two A-I_M/A-I_M molecules per particle, respectively (28). Under the same experimental conditions, apoA-I forms predominantly rHDL particles with a diameter of 9.6 nm, from which a 7.8-nm rHDL is derived (28), and other rHDL subspecies, including a 12.7-nm rHDL (28). When incorporated in these two rHDL, the A-I_M/A-I_M proved more effective than apoA-I in promoting cell cholesterol efflux (17) and less capable of activating the lecithin:cholesterol acyltransferase enzyme (16). In the present studies, we used limited proteolysis as a tool for investigating the conformation of A-I_M/A-I_M and apoA-I in the same small and large rHDL particles.

MATERIALS AND METHODS

Materials

A-I_M/A-I_M was expressed in the *E. Coli* and purified by conventional chromatographic procedures (27). The A-I_M/A-I_M batch used in the present study contained ~98% of A-I_M/A-I_M, as determined by SDS-PAGE (not shown). Normal apoA-I was purified from human blood plasma, as previously described (26). Before use, lyophilized A-I_M/A-I_M and apoA-I were dissolved in 20 mM phosphate buffer, pH 7.4, containing 6 M Gdn-HCl and extensively dialyzed against 10 mM Tris-HCl, pH 8.0, 150 mM NaCl, 1 mM NaN_3, and 0.01% EDTA (reconstitution buffer). Protein concentration of the stock solutions was assayed by amino acid analysis, performed on a Beckman 6300 amino acid analyzer after acidic hydrolysis of samples in 6 M HCl for 45 min at 155°C. L-α-palmitoyloleoylphosphatidylcholine (POPC), sodium cholate, elastase, and chymotrypsin were purchased from Sigma (St. Louis, MO). Trypsin was purchased from Boehringer (Indianapolis, IN).

Preparation and characterization of rHDL

Discoidal rHDL containing A-I_M/A-I_M or apoA-I and POPC, with a diameter of 7.8 or 12.5–12.7 nm, were prepared by the cholate dialysis technique (29), as previously described (28). The size of the particles was estimated by nondenaturing gradient gel electrophoresis (GGE) (28), using the Pharmacia Phast System (Pharmacia Biotech). The number of apolipoprotein molecules per rHDL particle was determined by cross-linking with dimethylsuberimidate (DMS) (27). Cross-linked samples were analyzed by SDS-PAGE on 4–10% acrylamide gradient slab gels, using the Tris-tricine buffer system of Schagger & Van Jagou (30) in a Mini Protean slab minigel apparatus (BioRad). Phospholipid content of rHDL was determined by an enzymatic method (31). Proteins were measured by the method of Lowry et al. (32), using bovine serum albumin as standard.

Circular dichroism (CD) spectra were recorded with a Jasco J500A spectropolarimeter at the constant temperature of 25°C. Molar mean residue ellipticity (θ) was expressed in degrees · cm^2 · dmol−1, and calculated as:

$$\theta = \theta_{obs} \cdot 115/10 \cdot l \cdot c \qquad \textit{Eq. 1)}$$

where θ_{obs} is the observed ellipticity in degrees, 115 is the mean residue molecular weight of the proteins, l is the optical path length in centimeters, and c is the protein concentration in grams/milliliter. All the spectra were baseline corrected. The α-helical content was calculated by the method of Chang, Wu, and Yang (33).

Limited proteolysis experiments

Reconstituted HDL containing A-I_M/A-I_M or apoA-I (about 0.1 mg/ml) were mixed with trypsin at the ratio of 1:50 (w/w) and incubated at 37°C. At various time intervals, aliquots were removed, SDS was added to obtain a final concentration of 4%, and samples were boiled for 2 min to terminate the reaction. The digestion products were stored at −20°C until analyzed by electrophoresis.

Analysis of proteolytic products

The digestion products were analyzed by SDS-PAGE on 10–16% acrylamide gradient slab gels, using the Tris-tricine buffer system (30). After electrophoresis, the peptide bands in the gels were either visualized with Coomassie Blue or electrophoretically transferred to polyvinylidene fluoride membranes. The membranes were then stained with Coomassie Blue, and the bands of interest were carefully cut from the membrane and subjected to automated sequence analysis on a pulsed-liquid sequencer (Applied Biosystems, Foster City, CA) equipped with a 120A Applied Biosystems PTH-analyzer.

The molecular weight of the trypsin fragments was determined by flight-mass spectrometry (MALDI/TOF-MS) using a Vestec Lasertec MALDI-TOF instrument (Perspective, Freburg, Germany) operating in a linear mode. Ions formed by a pulse ultraviolet laser beam (nitrogen laser, λ = 337 nm) were accelerated through 28 kV. The instrument was calibrated with bovine heart cytochrome *c* (MW = 12,327) and flagellin from *Bacillus subtilis* (MW = 32,626). The calibration proteins and the samples were dissolved in a solution of ferulic acid in 50% acetonitrile:50% water with trifluoroacetic acid 0.1%, to a final concentration of 50 pmoles/μl.

Western blotting

Some monoclonal antibodies (mAbs) used in these studies were a generous gift of Dr. G. R. Castro (A05, A17, A03, and

A44), and Drs. S. Marcovina and A. L. Catapano (A-I-11 and A-I-57); all mAbs have been previously described and characterized (34, 35). After trypsin digestion, the proteolytic fragments were separated by SDS-PAGE on 10–16% acrylamide gradient slab gels, and then electrophoretically transferred to membranes. After electroblotting, the membrane was incubated with albumin to prevent nonspecific binding. After blocking, the membrane was incubated with the primary antibody (mouse mAb) at 37°C for 1 h, washed, and incubated with the secondary antibody (goat anti-mouse IgG coupled to horseradish peroxidase). The immunocomplexes were detected using an enhanced chemiluminescence kit.

RESULTS

Upon interaction with POPC, A-I_M/A-I_M forms only two species of rHDL particles, with diameters of 7.8 and 12.5 nm (28). In the present studies we investigated the conformation of A-I_M/A-I_M in these two particles, in comparison with that of apoA-I in rHDL of comparable sizes. The rHDL preparations used here have the same characteristics of those used in the previous functional studies (16, 17). In particular, the 7.8- and 12.5-nm A-I_M/A-I_M rHDL contain one and two molecules of the dimer per particle, and display the same α-helical content of 62%. The 7.8- and 12.7-nm apoA-I rHDL contain two and three apoA-I molecules per particle, with an α-helical content of 61% and 71%.

Limited proteolysis of A-I_M/A-I_M and apoA-I rHDL

Limited proteolysis was used to investigate the conformation of A-I_M/A-I_M and apoA-I in rHDL particles. In initial experiments, each of the four rHDL was treated with proteolytic enzymes of differing specificities, chymotrypsin, trypsin, and elastase. The three proteases gave similar cleavage patterns (data not shown), i.e., consistent with previous findings (36, 37). Trypsin was used in further experiments.

The rHDL were subjected to tryptic digestion for various lengths of time, and the degree of protein degradation was estimated from the densitometry of SDS-PAGE gels (**Fig. 1**). Since equal amounts of protein were analyzed, the decrease in the intensity of the band corresponding to the intact protein truly reflects degradation of this protein. The extent of hydrolysis of apoA-I varies between small and large rHDL, such that apoA-I in the 7.8-nm rHDL is digested to a greater extent than apoA-I in the 12.7-nm rHDL (**Fig. 2**). ApoA-I in the small rHDL is degraded by ~50% after 6 h of proteolysis, with digestion being detectable at the earliest time points (Fig. 2). ApoA-I

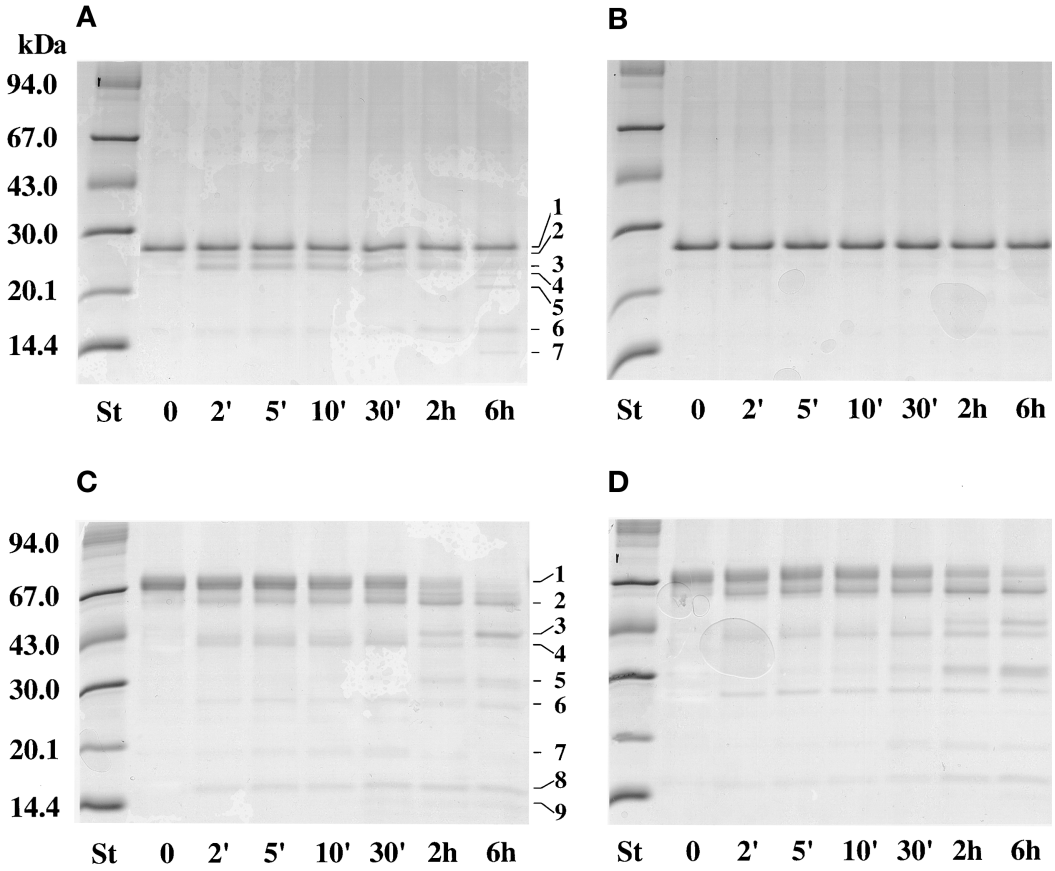

Fig. 1. Pattern of proteolysis of apoA-I (top) and A-I_M/A-I_M (bottom) rHDL particles by trypsin, as analyzed by SDS-PAGE. rHDL were incubated with trypsin at 37°C (enzyme:substrate ratio, 1:50); at various times, 10 μg of protein was removed, the reaction was terminated, and the digestion products were separated by SDS-PAGE. A: 7.8-nm apoA-I rHDL. B: 12.7-nm apoA-I rHDL. C: 7.8-nm A-I_M/A-I_M rHDL. D: 12.5-nm A-I_M/A-I_M rHDL.

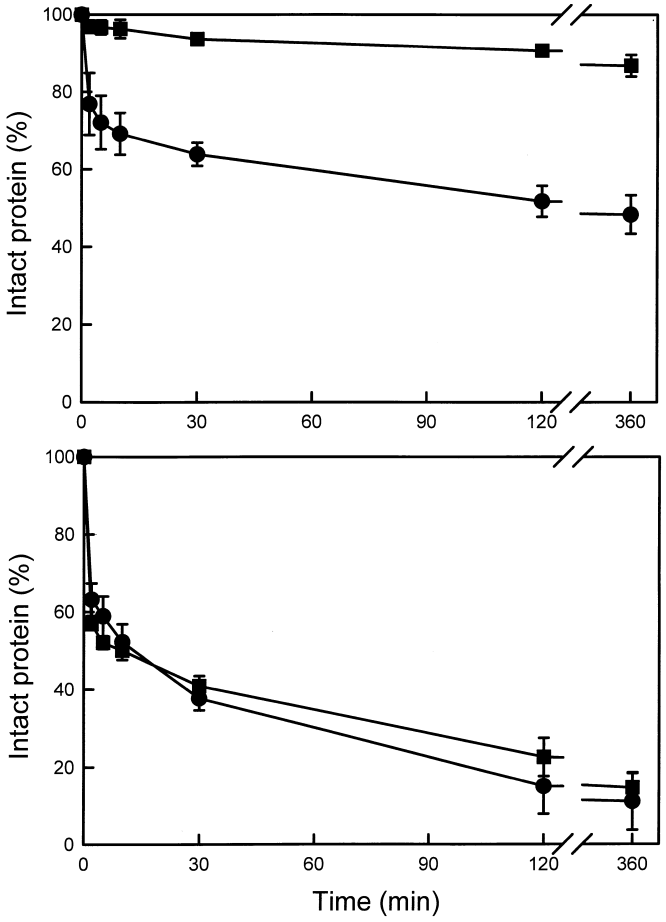

Fig. 2. Time-course of protein degradation in apoA-I (top) and A-I_M/A-I_M (bottom) rHDL of 7.8 nm (circles) and of 12.5–12.7 nm (squares) during incubation with trypsin. Proteolysis conditions are the same as in Fig. 1. The results are means ± SD of three different experiments with different rHDL preparation; SD within symbols are not shown.

in the large rHDL is instead resistant to proteolytic degradation, with ~90% of the protein remaining intact after prolonged digestion (Fig. 2).

Different from apoA-I, the protease susceptibility of A-I_M/A-I_M in 7.8- and 12.5-nm rHDL particles is remarkably similar (Fig. 1), suggesting that A-I_M/A-I_M adopts a similar conformation in small and large rHDL. This result agrees with our previous observations that A-I_M/A-I_M has the same secondary and tertiary structure when incorporated into small or large rHDL (28). It is noteworthy that A-I_M/A-I_M is definitely more susceptible to proteolytic digestion than apoA-I, as indicated by its pronounced degradation at shorter times. Fifty percent of A-I_M/A-I_M is already degraded after 10 min of proteolysis, with only ~10% of the protein remaining intact after 6 h of incubation (Fig. 2). By contrast, the protease susceptibility of the monomeric A-I_M in rHDL is remarkably similar to that of apoA-I (not shown).

Particle integrity over the time course of the proteolysis experiment was assessed by nondenaturing gradient gel electrophoresis. No changes in rHDL particle size are detected in control incubations without trypsin. Both apoA-I rHDL particles are stable over the 6 h of proteolysis. A-I_M/A-I_M rHDL do not change in size during the first 30 min of incubation, despite a significant protein degradation (~40% of A-I_M/A-I_M remaining intact); the particles become more heterogeneous at 2 h, and some protein dissociates from rHDL after 6 h of proteolysis.

Identification of cleavage sites

At the same time intervals that protein degradation was estimated, the cleavage products generated by trypsin digestion were separated by SDS-PAGE (Fig. 1). The identification of the cleavage sites in apoA-I and of A-I_M/A-I_M was achieved by *i*) immunoblotting of SDS-PAGE gels with a panel of mAbs directed against epitopes distributed all along the apoA-I sequence (**Figs. 3** and **4**), *ii*) N-terminal sequencing of proteolytic fragments isolated by SDS-PAGE (**Tables 1** and **2**), and *iii*) determination of the molecular mass of the digestion products by mass spectrometry (Tables 1 and 2).

Treatment of 7.8-nm apoA-I rHDL with trypsin yields six additional bands by SDS-PAGE, corresponding to polypeptides with molecular masses ranging between 24.9 and 13.2 kDa (Fig. 1, Table 2). All these products are recognized by mAbs 4H1 and AO5 (Fig. 4), which bind to the apoA-I sequences Glu^2-Trp^8 and Ser^{25}-Leu^{82} (34) (Fig. 3), indicating that all peptides contain the apoA-I N-terminus, as proved by N-terminal sequencing (Table 1). Therefore, no cleavage occurs in the amino-terminal region of apoA-I, when the protein is bound to POPC in rHDL. Bands 2 to 4 on SDS-PAGE react with all the tested mAbs (Fig. 4), suggesting that they correspond to peptides lacking different portions of the C-terminus, which is not recognized by any antibody. The molecular masses of these large fragments, and of the small complementary peptides, are consistent with cleavage at residues Arg^{215}, Lys^{195}, and Arg^{188} (Table 1). Band 5 reacts with mAbs mapping to the amino-terminal and central regions of apoA-I, and it corresponds to the peptide cleaved at Arg^{160} (Table 1). Band 6 reacts with mAbs recognizing the N-terminus of apoA-I (4H1, A05 and A-I-11) (Fig. 4). Molecular mass and sequence analysis indicate this band indeed includes two distinct peptides, of 14.1 and 13.9 kDa, with N-terminal sequences starting at Val^{119} and Asp^1, respectively (Table 1). Therefore, band 6 con-

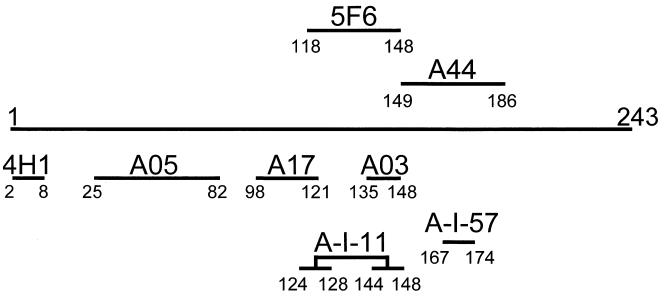

Fig. 3. Epitope map of apoA-I. The positions of epitopes recognized by the mAbs used in the present study have been previously defined and described (35, 36). The names of mAbs are placed above the solid line bars, which represent the sequence of apoA-I recognized by the various mAbs.

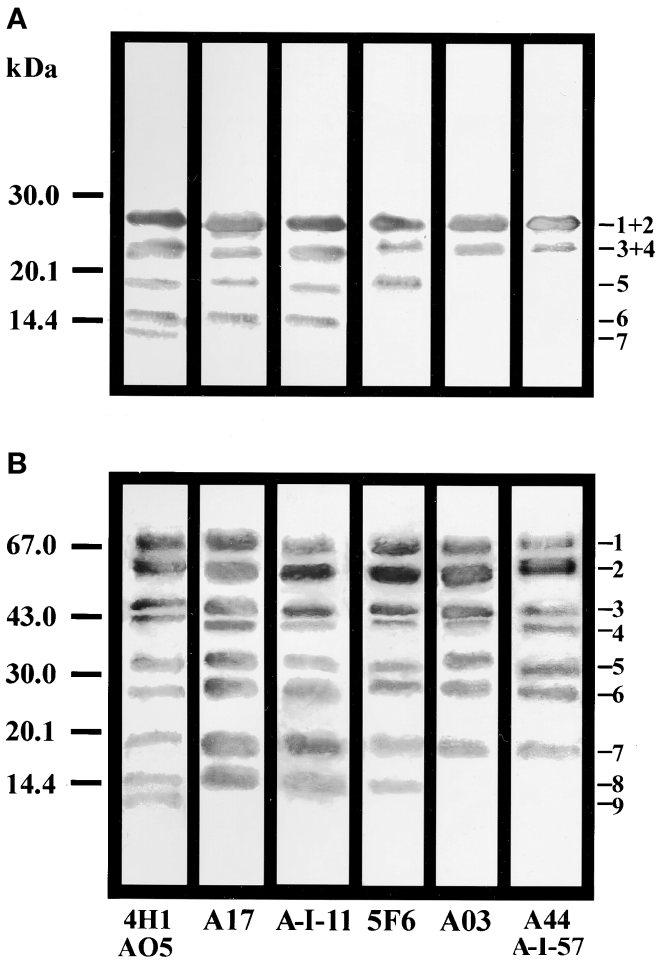

Fig. 4. Western-blotting analysis with different mAbs of the proteolytic fragments generated by protein digestion for 6 h of the 7.8-nm apoA-I rHDL (A) and the 7.8-nm A-I_M/A-I_M rHDL (B). Bands are identified by the same numbers reported in Fig. 1 and Tables 1 and 2. Note that the apoA-I proteolytic fragments corresponding to bands 1 and 2 and 3 and 4 are not resolved in the immunoblotting.

tains the complementary peptides generated by cleavage of apoA-I at Lys^{118}, which cannot be solved owing to insufficient resolution by SDS-PAGE. The Val^{119}-Gln^{243} fragment may be generated early during digestion, being further

TABLE 1. Identity of fragments obtained by proteolysis of 7.8-nm apoA-I rHDL

SDS-PAGE Band[a]	Molecular Mass	N-Terminal Sequence	Fragment
	KDa		
1	28.1	Asp-Glu-Pro-Pro . . .	Asp^1-Gln^{243}
2	24.9	Asp-Glu-Pro-Pro . . .	Asp^1-Arg^{215}
3	22.7	Asp-Glu-Pro-Pro . . .	Asp^1-Lys^{195}
4	21.9	Asp-Glu-Pro-Pro . . .	Asp^1-Arg^{188}
5	18.8	Asp-Glu-Pro-Pro . . .	Asp^1-Arg^{160}
6	14.1	Val-Glu-Pro-Leu . . .	Val^{119}-Gln^{243}
	13.9	Asp-Glu-Pro-Pro . . .	Asp^1-Lys^{118}
7	11.0	Asp-Glu-Pro-Pro . . .	Asp^1-Lys^{94}

[a] Labels of fragments refer to their corresponding band position on SDS-PAGE, which can be found in Fig. 1. In cases where more than one sequence is present, comigration of fragments is assumed due to non-optimal resolution on SDS-PAGE.

TABLE 2. Identity of fragments obtained by proteolysis of 7.8- and 12.5-nm A-I_M/A-I_M rHDL

SDS-PAGE Band[a]	Molecular Mass	N-Terminal Sequence	Fragment
	KDa		
1	56.0	Asp-Glu-Pro-Pro . . .	Asp^1-Gln^{243}/Asp^1-Gln^{243}
2	49.7	Asp-Glu-Pro-Pro . . .	Asp^1-Arg^{215}/Asp^1-Arg^{215}
3	45.3	Asp-Glu-Pro-Pro . . .	Asp^1-Lys^{195}/Asp^1-Lys^{195}
4	43.7	Asp-Glu-Pro-Pro . . .	Asp^1-Arg^{188}/Asp^1-Arg^{188}
5	32.8	Asp-Glu-Pro-Pro . . . Ala-Lys-Val-Gln . . .	Asp^1-Arg^{188}/Ala^{95}-Arg^{188}
6	27.3	Ala-Glu-Leu-Gln . . .	Ala^{124}-Gln^{243}/Ala^{124}-Gln^{243}
7	18.8	Asp-Glu-Pro-Pro . . .	Asp^1-Arg^{160}
	18.5	Thr-His-Leu-Ala . . .	Thr^{161}-Gln^{243}/Thr^{161}-Gln^{243}
8	14.5	Asp-Glu-Pro-Pro . . .	Asp^1-Arg^{123}
9	11.0	Asp-Glu-Pro-Pro . . .	Asp^1-Lys^{94}

[a] Labels of fragments refer to their corresponding band position on SDS-PAGE, which can be found in Fig. 1. In cases where more than one sequence is present, comigration of fragments is assumed due to non-optimal resolution on SDS-PAGE.

degraded toward its carboxy-terminal end, with formation of smaller fragments. Indeed, immunoreactivity of band 6 with mAbs mapped to the central portion of apoA-I (A44 and A-I-57) is observed at the earliest (not shown) but not latest (Fig. 4) time points after the addition of protease.

All together, immunoblotting, N-terminal sequencing, and mass spectrometry show that apoA-I in the 7.8-nm rHDL is cleaved by trypsin at Lys^{94}, Lys^{118}, Arg^{160}, Arg^{188}, Lys^{195}, and Arg^{215} (Table 1, **Fig. 5**). The Asp^1-Arg^{215}, Asp^1-Lys^{195}, and Asp^1-Lys^{118} peptides (bands 2, 3, and 6, respectively, in Fig. 1) are formed immediately after the digestion starts; the three other fragments, Asp^1-Arg^{188}, Asp^1-Arg^{160}, and Asp^1-Lys^{94} (bands 4, 5, and 7, respectively, in Fig. 1), appear later during digestion, indicating a lower exposure of the corresponding cleavage sites to the protease or a formation secondary to first cleavages. Although the proteolysis experiments were not designed to evaluate the kinetics of the degradation process, the identification of earlier and later cleavage sites is consistent with the apparently multiphases decay of the intact protein (Fig. 2).

As indicated above, apoA-I in the 12.7-nm rHDL is much more resistant to trypsin digestion than in the small rHDL. A clear-cut visualization of the proteolytic products can be achieved only after prolonged digestion (24 h, not shown), when seven bands can be identified by SDS-PAGE. The proteolytic products have been characterized by N-terminal

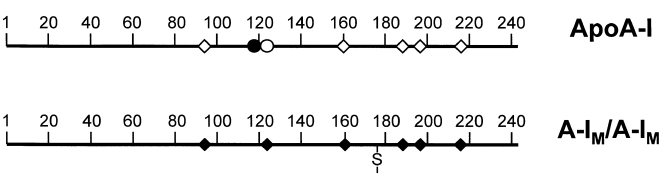

Fig. 5. Linear sequence maps of apoA-I (top) and A-I_M/A-I_M (bottom) showing the observed proteolytic cleavage sites. The open diamonds identify cleavage sites common to apoA-I in both small and large rHDL; the circles identify sites unique to apoA-I in small (closed circle) or large (open circle) rHDL. The A-I_M/A-I_M displays the same cleavage sites in both small and large rHDL, which are identified by closed diamonds.

sequencing and mass spectrometry. Five of the generated peptides (bands 2–5 and 7) are identical to those obtained after digestion of 7.8-nm apoA-I rHDL. By contrast, band 6 includes two peptides that are different from those found in degraded 7.8-nm apoA-I rHDL; these proteolytic products, with masses of 14.5 and 13.6 kDa, correspond to the Asp^{1}-Arg^{123} and the complementary Ala^{124}-Gln^{243} peptides (Fig. 5). Therefore, cleavage in the central portion of apoA-I occurs at distinct sites in small (Lys^{118}) and large (Arg^{123}) rHDL particles.

Trypsin cleavage of A-I_M/A-I_M in 7.8- and 12.5-nm rHDL particles gives the same eight additional bands by SDS-PAGE, corresponding to proteolytic fragments ranging in molecular mass from 49.7 to 11.0 kDa (Fig. 1, Table 2). The band with an approximate molecular mass of 19 kDa (band 7) indeed includes two distinct products, with masses of 18.8 and 18.5 kDa, as determined by N-terminal sequencing (Table 2). Therefore, nine large peptides are generated by digestion of A-I_M/A-I_M with trypsin. Bands 2–5 on SDS-PAGE react with all the mAbs (Fig. 4), suggesting that they correspond to peptides lacking different portions of the carboxy-terminal region of the protein. Three of these peptides, of 49.7 kDa (band 2), 45.3 kDa (band 3), and 43.7 kDa (band 4), contain an intact N-terminus and the interchain disulfide bridge at Cys^{173}; the molecular masses of these fragments, and of the small complementary peptides, are consistent with cleavage at residues Arg^{215}, Lys^{195} and Arg^{188} (Table 2). The 43.7 homodimer (band 4) is an intermediate, and is further cleaved at Lys^{94} of one chain to generate the 32.8-kDa heterodimer (band 5) and the complementary Asp^{1}-Lys^{94} peptide (band 9) (Table 2). Band 6 corresponds to a disulfide-linked peptide with molecular mass of 27.3 kDa and the Ala^{124}-Gln^{243} sequence (Table 2); this peptide, therefore, should not react with mAbs recognizing the N-terminus (4H1 and AO5). Some immunoreactivity is, however, found on immunoblotting (Fig. 4), possibly due to the co-migrating A-I_{Milano} monomer, which is a contaminant (<2%) of the A-I_M/A-I_M preparation; some intact N-terminus is indeed detected by sequencing. Band 7 is recognized by all the mAbs and, indeed, consists of two peptides with N-terminal sequences starting at Asp^{1} and Thr^{161} (Table 2). Therefore, cleavage in the central portion of A-I_M/A-I_M, at Arg^{123} and Arg^{160}, gives two monomeric peptides of 18.8 kDa (band 7) and 14.5 kDa (band 8), containing the intact N-terminus, together with the complementary homodimers of 27.3 kDa (band 6) and 18.5 kDa (band 7). Five primary cleavage sites, located at Arg^{123}, Arg^{160}, Arg^{188}, Lys^{195}, and Arg^{215}, and one secondary cleavage site at Lys^{94}, are thus present in the lipid-bound A-I_M/A-I_M (Fig. 5). As observed for apoA-I, the presence of earlier and later cleavage sites is consistent with the multiphases kinetics of intact protein degradation (Fig. 2).

DISCUSSION

Our previous studies (28) have shown that, upon interaction with phospholipids, A-I_M/A-I_M forms only two species of rHDL, with diameters of 7.8 and 12.5 nm, containing one or two A-I_M/A-I_M molecules per particle, respectively, whereas apoA-I forms rHDL particles of increasing size with increasing lipid:protein ratio in the incubation mixture. We hypothesized that the introduction of an interchain disulfide bridge in the A-I_M/A-I_M protein restricts rHDL particle size heterogeneity by restraining the intrinsic structural adaptability of the wild-type monomeric apoA-I. In the present studies, we have relied on limited proteolysis to probe the conformation of A-I_M/A-I_M on the surface of the two rHDL particles, in comparison with that of wild-type apoA-I in rHDL of comparable size. Limited proteolysis has been widely used to study the domain structure of proteins (38), due to the correspondence between accessibility to the protease and the lack of an organized secondary structure. Proteolytic digestion of a globular protein is expected to occur at surface loops and random segments, or at flexible hinges between protein domains, rather than inside rigid elements of secondary structure, such as helices or pleated sheets (38). The present work demonstrates that (i) apoA-I in small rHDL is remarkably more sensitive to proteolytic digestion than in large rHDL; (ii) A-I_M/A-I_M in small and large rHDL shows the same susceptibility to proteolysis, being much more sensitive to digestion than apoA-I; and (iii) the amino-terminal region of both apoA-I and A-I_M/A-I_M is resistant to proteolysis, with the cleavage sites located in the central and carboxy-terminal portions of the molecules.

ApoA-I in small rHDL was definitely more susceptible to proteolytic digestion than in large rHDL. The observation of a distinct susceptibility to proteases of apoA-I in rHDL of different size is in agreement with previous results of Dalton and Swaney (36), who observed an inverse relationship between the size of rHDL and the extent of apoA-I degradation, and with the more rapid denaturation of apoA-I in small than large particles (39). Furthermore, Kunitake et al. (40) showed that the apoA-I of plasma-derived pre-β-migrating HDL, somewhat comparable to the present 7.8-nm rHDL particles in terms of size and surface charge (indeed, all the rHDL used in this study migrate in pre-β position), displays an enhanced sensitivity to proteolysis than apoA-I of α-migrating, larger HDL. All together, these findings fully support the concept, originally developed from spectroscopic (22) and epitope mapping (19) studies, of a distinct conformation of apoA-I in rHDL of different size that contain the same number of apoA-I molecules.

The change in conformation caused by variations in apoA-I rHDL size seems to involve a hinged domain, that is, a mobile portion of the molecule constituted by a pair of consecutive amphipathic helices, which can exist either bound to lipids in the large rHDL or looping out of the small rHDL into the aqueous milieu (19). This concept, originally developed on the basis of the picket-fence model of apoA-I structural organization in rHDL (19), may also adapt to the alternative belt model (20, 21). It is reasonable that, once dissociated from the lipid core of the small rHDL, this hinged domain loses its helical structure, as indicated by the reduced α-helical content of small than large

rHDL particles (22, 28). Two regions, encompassing the helices 4 and 5 (residues 99–143), or 5 and 6 (residues 121–165) of apoA-I (11), have been proposed to form the hinge (19, 41), but its exact position has never been clearly demonstrated. The present work has identified distinct cleavage sites at Lys^{118} and Arg^{123} in small and large apoA-I rHDL, respectively, indicating a different conformation of this portion of apoA-I in the two rHDL particles, therefore supporting the concept that is indeed the 99–143 region that forms the hinge.

Although 7.8- and 12.7-nm apoA-I rHDL display a distinct susceptibility to proteolytic digestion, A-I_M/A-I_M shows the same sensitivity to proteases when bound to small or large rHDL particles. This is in agreement with the almost identical spectral properties of A-I_M/A-I_M in the same small and large rHDL (28), and indicates that A-I_M/A-I_M has a limited structural plasticity compared with apoA-I. The generation of apoA-I rHDL particles of different sizes and containing a constant number of apoA-I molecules per particle has been explained by the conformational flexibility of the hinged domain in the central portion of apoA-I (19). In the case of both small and large A-I_M/A-I_M rHDL, cleavage in the central portion of the A-I_M/A-I_M molecule occurs at the same position as in the 12.7-nm apoA-I rHDL, where the hinged domain is in the lipid-bound conformation (19). This indicates that also in the two A-I_M/A-I_M rHDL, the hinged domain is in contact with the lipid bilayer and assumes helical structure. Because the two A-I_M/A-I_M rHDL display an α-helical content similar to the 7.8-nm apoA-I rHDL and lower than the 12.7-nm apoA-I rHDL (28), a portion of A-I_M/A-I_M, distinct from the hinged domain, is not in contact with lipids and loses the α-helical structure.

The present results can be adapted to both models proposed for the structure of apoA-I around the periphery of the rHDL. The belt model for rHDL discs with a diameter of 10–10.5 nm and containing two apoA-I molecules per particle, describes apoA-I organization in terms of the X-ray structure (14), with apoA-I forming a pair of continuous amphipathic helices parallel to the plane of the disc (21). In the picket-fence model for rHDL containing two or three apoA-I molecules per particle, the amphipathic apoA-I helices arrange into tightly packed antiparallel segments, oriented perpendicular to the plane of the disc (22, 23). Both picket-fence and belt models for A-I_M/A-I_M rHDL have been recently proposed (1, 42). The present experiments were not designed to distinguish between the two models, and the results do not favor either hypothesis. It is noteworthy that, although the picket-fence model (1) is easily adaptable to the small and large rHDL containing one and two A-I_M/A-I_M molecules per particle, the proposed belt model of a 9–10-nm A-I_M/A-I_M rHDL (42) appears incompatible with the experimentally generated rHDL sizes (28). Whether it is organized in the picket-fence or belt manner, the A-I_M/A-I_M adopts a conformation that is different from that of apoA-I, with the C-terminal portion being more susceptible to proteolytic degradation. It seems reasonable to speculate that the disulfide bridge in A-I_M/A-I_M sets a structural constraint that forcedly displaces out of the discs the C-terminal residues of A-I_M/A-I_M, starting approximately at Ala^{187} (11). This would form a distinctly folded domain, not detectable in apoA-I, that, not involved in lipid-binding, would rapidly lose its helical structure, i.e., consistent with the circular dichroism data (28).

Cleavage sites in apoA-I and A-I_M/A-I_M were located in the central and carboxy-terminal portions of the protein with no cleavage occurring in the amino-terminal domain. These results are consistent with those of previous studies on apoA-I proteolysis in homogeneous, POPC-containing rHDL (36, 37), but differ from those of Lins et al. (43), who showed cleavage by trypsin and other proteases at residues 43–48 of apoA-I in DMPC-containing complexes. Roberts et al. (44) recently reported that the oxidative state of apoA-I is a major determinant of protein conformation and protease susceptibility: oxidation of two methionines at residues 112 and 148 in the primary sequence switches the protease cleavage sites from the N-terminus to the central and carboxy-terminal regions of the protein. In the present study, the lack of cleavage in the amino-terminal region of both apoA-I and A-I_M/A-I_M is not due to protein oxidation, as demonstrated by determination of protein masses by mass spectrometry (apoA-I: 28,078 Da; A-I_M/A-I_M: 56,050 Da). These somewhat conflicting results might be due to differences in the size and composition of rHDL, in the rHDL purification procedure used, and/or in the proteolytic conditions.

In conclusion, the introduction of an interchain disulfide bridge in apoA-I remarkably affects the conformation of the protein when bound to lipids, with generation of a unique C-terminal domain. The specific conformation of the lipid-bound A-I_M/A-I_M would account for the delayed in vivo catabolism (45), and for the peculiar properties of this protein in lipoprotein metabolism (16, 17, 46) and atherosclerosis protection (1).

We are most grateful to Dr. H. Ageland (Pharmacia, Sweden) for providing the recombinant A-I_M/A-I_M. We thank Drs. G. R. Castro, S. Marcovina and A. L. Catapano for providing the monoclonal antibodies.

Manuscript received 31 July 2000 and in revised form 3 January 2001.

REFERENCES

1. Sirtori, C. R., L. Calabresi, and G. Franceschini. 1999. Recombinant apolipoproteins for the treatment of vascular diseases. *Atherosclerosis.* **142:** 29–40.
2. Duverger, N., H. Kruth, F. Emmanuel, J. M. Caillaud, C. Viglietta, G. R. Castro, A. Tailleux, C. Fievet, J. C. Fruchart, L. M. Houdebine, P. Denefle, and G. Castro. 1996. Inhibition of atherosclerosis development in cholesterol-fed human apolipoprotein A-I-transgenic rabbits. *Circulation.* **94:** 713–717.
3. Paszty, C., N. Maeda, J. Verstuyft, and E. M. Rubin. 1994. Apolipoprotein AI transgene corrects apolipoprotein E deficiency-induced atherosclerosis in mice. *J. Clin. Invest.* **94:** 899–903.
4. Rubin, E. M., R. M. Krauss, E. A. Spangler, J. G. Verstuyft, and S. M. Clift. 1991. Inhibition of early atherogenesis in transgenic mice by human apolipoprotein AI. *Nature.* **353:** 265–267.
5. De Geest, B., Z. Zhao, D. Collen, and P. Holvoet. 1997. Effects of adenovirus-mediated human apo A-I gene transfer on neointima formation after endothelial denudation in apo E-deficient mice. *Circulation.* **96:** 4349–4356.

6. Franceschini, G., J. P. Werba, and L. Calabresi. 1994. Drug control of reverse cholesterol transport. *Pharmacol. Ther.* **61:** 289–324.
7. Yui, Y., T. Aoyama, H. Morishita, M. Takahashi, Y. Takatsu, and C. Kawai. 1988. Serum prostacyclin stabilizing factor is identical to apolipoprotein A-I (Apo A-I). A novel function of Apo A-I. *J. Clin. Invest.* **82:** 803–807.
8. Saku, K., M. Ahmad, P. Glas-Greenwalt, and M. L. Kashyap. 1985. Activation of fibrinolysis by apolipoproteins of high density lipoproteins in man. *Thromb. Res.* **39:** 1–8.
9. Calabresi, L., G. Franceschini, C. R. Sirtori, A. de Palma, M. Saresella, P. Ferrante, and D. Taramelli. 1997. Inhibition of VCAM-1 expression in endothelial cells by reconstituted high density lipoproteins. *Biochem. Biophys. Res. Commun.* **238:** 61–65.
10. Brewer, H. B., Jr., T. Fairwell, A. Larue, R. Ronan, A. Houser, and T. J. Bronzert. 1978. The amino acid sequence of human apoA-I, an apolipoprotein isolated from high density lipoprotein. *Biochem. Biophys. Res. Commun.* **80:** 623–630.
11. Narayanaswami, V., and R. O. Ryan. 2000. Molecular basis of exchangeable apolipoprotein function. *Biochim. Biophys. Acta.* **1483:** 15–36.
12. Nolte, R. T., and D. Atkinson. 1992. Conformational analysis of apolipoprotein A-I and E-3 based on primary sequence and circular dichroism. *Biophys. J.* **63:** 1221–1239.
13. Segrest, J. P., M. K. Jones, H. De Loof, C. G. Brouillette, Y. V. Venkatachalapathi, and G. M. Anantharamaiah. 1992. The amphipathic helix in the exchangeable apolipoproteins: a review of secondary structure and function. *J. Lipid Res.* **33:** 141–166.
14. Borhani, D. W., D. P. Rogers, J. A. Engler, and C. G. Brouillette. 1997. Crystal structure of truncated human apolipoprotein A-I suggests a lipid-bound conformation. *Proc. Natl. Acad. Sci. USA.* **94:** 12291–12296.
15. Jonas, A. 1986. Reconstitution of high-density lipoproteins. *Methods Enzymol.* **128:** 553–582.
16. Calabresi, L., G. Franceschini, A. Burkybile, and A. Jonas. 1997. Activation of lecithin cholesterol acyltransferase by a disulfide-linked apolipoprotein A-I dimer. *Biochem. Biophys. Res. Commun.* **232:** 345–349.
17. Calabresi, L., M. Canavesi, F. Bernini, and G. Franceschini. 1999. Cell cholesterol efflux to reconstituted high-density lipoproteins containing the apolipoprotein A-I_{Milano} dimer. *Biochemistry.* **38:** 16307–16314.
18. Jonas, A. 1991. Lecithin-cholesterol acyltransferase in the metabolism of high-density lipoproteins. *Biochim. Biophys. Acta.* **1084:** 205–220.
19. Calabresi, L., Q. H. Meng, G. R. Castro, and Y. L. Marcel. 1993. Apolipoprotein A-I conformation in discoidal particles: evidence for alternate structures. *Biochemistry.* **32:** 6477–6484.
20. Koppaka, V., L. Silvestro, J. A. Engler, C. G. Brouillette, and P. H. Axelsen. 1999. The structure of human lipoprotein A-I. Evidence for the "belt" model. *J. Biol. Chem.* **274:** 14541–14544.
21. Segrest, J. P., M. K. Jones, A. E. Klon, C. J. Sheldahl, M. Hellinger, H. De Loof, and S. C. Harvey. 1999. A detailed molecular belt model for apolipoprotein A-I in discoidal high density lipoprotein. *J. Biol. Chem.* **274:** 31755–31758.
22. Jonas, A., K. E. Kezdy, and J. H. Wald. 1989. Defined apolipoprotein A-I conformations in reconstituted high density lipoprotein discs. *J. Biol. Chem.* **264:** 4818–4824.
23. Phillips, J. C., W. Wriggers, Z. Li, A. Jonas, and K. Schulten. 1997. Predicting the structure of apolipoprotein A-I in reconstituted high-density lipoprotein disks. *Biophys. J.* **73:** 2337–2346.
24. Franceschini, G., C. R. Sirtori, A. Capurso, K. H. Weisgraber, and R. W. Mahley. 1980. A-I_{Milano} apoprotein. Decreased high density lipoprotein cholesterol levels with significant lipoprotein modifications and without clinical atherosclerosis in an Italian family. *J. Clin. Invest.* **66:** 892–900.
25. Weisgraber, K. H., S. C. Rall, Jr., T. P. Bersot, R. W. Mahley, G. Franceschini, and C. R. Sirtori. 1983. Apolipoprotein AI_{Milano}. Detection of normal AI in affected subjects and evidence for a cysteine for arginine substitution in the variant AI. *J. Biol. Chem.* **258:** 2508–2513.
26. Franceschini, G., G. Vecchio, G. Gianfranceschi, D. Magani, and C. R. Sirtori. 1985. Apolipoprotein A-I_{Milano}. Accelerated binding and dissociation from lipids of a human apolipoprotein variant. *J. Biol. Chem.* **260:** 16321–16325.
27. Calabresi, L., G. Vecchio, R. Longhi, E. Gianazza, G. Palm, H. Wadensten, A. Hammarstrom, A. Olsson, A. Karlstrom, T. Sejlitz, H. Ageland, C. R. Sirtori, and G. Franceschini. 1994. Molecular characterization of native and recombinant apolipoprotein A-I_{Milano} dimer. The introduction of an interchain disulfide bridge remarkably alters the physicochemical properties of apolipoprotein A-I. *J. Biol. Chem.* **269:** 32168–32174.
28. Calabresi, L., G. Vecchio, F. Frigerio, L. Vavassori, C. R. Sirtori, and G. Franceschini. 1997. Reconstituted high-density lipoproteins with a disulfide-linked apolipoprotein A-I dimer: evidence for restricted particle size heterogeneity. *Biochemistry.* **36:** 12428–12433.
29. Matz, C. E., and A. Jonas. 1982. Micellar complexes of human apolipoprotein A-I with phosphatidylcholines and cholesterol prepared from cholate-lipid dispersions. *J. Biol. Chem.* **257:** 4535–4540.
30. Schagger, H., and G. vonJagow. 1987. Tricine-sodium dodecyl sulfate-polyacrylamide gel electrophoresis for the separation of proteins in the range from 1 to 100kDa. *Anal. Biochem.* **166:** 368–379.
31. Takayama, M., S. Itoh, T. Nagasaki, and I. Tanimizu. 1977. A new enzymatic method for determination of serum choline-containing phospholipids. *Clin. Chim. Acta.* **79:** 93–96.
32. Lowry, O. H., N. J. Rosebrough, A. L. Farr, and R. J. Randall. 1951. Protein measurement with the Folin phenol reagent. *J. Biol. Chem.* **193:** 265–275.
33. Chang, C. T., C. C. Wu, and J. T. Yang. 1978. Circular dichroic analysis of protein conformation: inclusion of the β-turns. *Anal. Biochem.* **91:** 13–31.
34. Marcel, Y. L., P. R. Provost, H. Koa, E. Raffai, N. V. Dac, J. C. Fruchart, and E. Rassart. 1991. The epitopes of apolipoprotein A-I define distinct structural domains including a mobile middle region. *J. Biol. Chem.* **266:** 3644–3653.
35. Marcovina, S. M., S. Fantappie, A. Zoppo, G. Franceschini, and A. L. Catapano. 1990. Immunochemical characterization of six monoclonal antibodies to human apolipoprotein A-I: epitope mapping and expression. *J. Lipid. Res.* **31:** 375–384.
36. Dalton, M. B., and J. B. Swaney. 1993. Structural and functional domains of apolipoprotein A-I within high density lipoproteins. *J. Biol. Chem.* **268:** 19274–19283.
37. Ji, Y., and A. Jonas. 1995. Properties of an N-terminal proteolytic fragment of apolipoprotein AI in solution and in reconstituted high density lipoproteins. *J. Biol. Chem.* **270:** 11290–11297.
38. Fontana, A., G. Fassina, C. Vita, D. Dalzoppo, M. Zamai, and M. Zambonin. 1986. Correlation between sites of limited proteolysis and segmental mobility in thermolysin. *Biochemistry.* **25:** 1847–1851.
39. Jonas, A., J. H. Wald, K. L. Toohill, E. S. Krul, and K. E. Kezdy. 1990. Apolipoprotein A-I structure and lipid properties in homogeneous, reconstituted spherical and discoidal high density lipoproteins. *J. Biol. Chem.* **265:** 22123–22129.
40. Kunitake, S. T., G. C. Chen, S-F. Kung, J. W. Schilling, D. A. Hardman, and J. P. Kane. 1990. Pre-beta high density lipoportein. Unique disposition of apolipoprotein A-I increases suceptibility to proteolysis. *Arteriosclerosis.* **10:** 25–30.
41. Bergeron, J., P. G. Frank, D. Scales, Q. H. Meng, G. R. Castro, and Y. L. Marcel. 1995. Apolipoprotein A-I conformation in reconstituted discoidal lipoproteins varying in phospholipid and cholesterol content. *J. Biol. Chem.* **270:** 27429–27438.
42. Klon, A. E., M. K. Jones, J. P. Segrest, and S. C. Harvey. 2000. Molecular belt models for the apolipoprotein A-I Paris and Milano mutations. *Biophys. J.* **79:** 1679–1685.
43. Lins, L., S. Piron, K. Conrath, B. Vanloo, R. Brasseur, M. Rosseneu, J. Baert, and J. M. Ruysschaert. 1993. Enzymatic hydrolysis of reconstituted dimyristoylphosphatidylcholine-apo A-I complexes. *Biochim. Biophys. Acta.* **1151:** 137–142.
44. Roberts, L. M., M. J. Ray, T. W. Shih, E. Hayden, M. M. Reader, and C. G. Brouillette. 1997. Structural analysis of apolipoprotein A-I: limited proteolysis of methionine-reduced and -oxidized lipid-free and lipid-bound human apo A-I. *Biochemistry.* **36:** 7615–7624.
45. Roma, P., R. E. Gregg, M. S. Meng, R. Ronan, L. A. Zech, G. Franceschini, C. R. Sirtori, and H. B. Brewer, Jr. 1993. In vivo metabolism of a mutant form of apolipoprotein A-I, apo A- I_{Milano}, associated with familial hypoalphalipoproteinemia. *J. Clin. Invest.* **91:** 1445–1452.
46. Franceschini, G., L. Calabresi, C. Tosi, G. Gianfranceschi, C. R. Sirtori, and A. V. Nichols. 1990. Apolipoprotein A-I_{Milano}. Disulfide-linked dimers increase high density lipoprotein stability and hinder particle interconversion in carrier plasma. *J. Biol. Chem.* **265:** 12224–12231.